RESEARCH FRONT

CSIRO PUBLISHING

Aust. J. Chem. **2012**, *65*, 1384–1389
http://dx.doi.org/10.1071/CH12085

Communication

Highly Sheared Anti-Parallel Dipolar Carbonyl···Carbonyl Interaction in the Crystal Packing of Strapped Crown-3-Pyromellitimide

Ethan Nam Wei Howe,[A] *Mohan Bhadbhade,*[B] *and Pall Thordarson*[A,C]

[A]School of Chemistry, The University of New South Wales, Sydney, NSW 2052, Australia.
[B]Mark Wainwright Analytical Centre, The University of New South Wales, Sydney, NSW 2052, Australia.
[C]Corresponding author. Email: p.thordarson@unsw.edu.au

Non-covalent dipolar interactions between pairs of carbonyls have been demonstrated to play a significant role in the crystal packing and formation of supramolecular structural architecture of small organic molecules. Under high dilution, the strapped crown-3-pyromellitimide **4** and macrocyclic crown-6-bispyromellitimide **5** were synthesised in concert and demonstrated selective molecular recognition towards Na^+ and K^+, respectively. The molecular structure of strapped crown-3-pyromellitimide **4** was solved using X-ray crystallography and an unusual highly sheared anti-parallel dipolar carbonyl···carbonyl interaction was observed in the crystal packing. The intermolecular interaction has a torsion angle of 44.1°, and deviates from the three idealised motifs reported in literature. This finding further highlights the importance and versatility of dipolar carbonyl···carbonyl interaction in the crystal packing of organic molecules.

Manuscript received: 8 February 2012.
Manuscript accepted: 21 May 2012.
Published online: 28 June 2012.

Introduction

The chemistry of non-covalent intermolecular interactions, commonly known as supramolecular chemistry has greatly influenced and improved our understanding in the molecular recognition processes of self-assembly and host-guest chemistry.[1] Due to the prevalent focus on the hydrogen bonding, other intermolecular interactions have frequently been overlooked despite the important role they play in supramolecular systems. One example is the dipolar carbonyl···carbonyl interaction which was found to be ubiquitous in both chemical and biological molecular recognition processes.[2] This includes applications in crystal engineering,[3] ligand-based medicinal drug design,[4] and the synthesis of supramolecular metal-organic frameworks,[5] helices,[6] and columnar structures.[7]

Dipolar carbonyl···carbonyl interactions were first reported by Bolton[8,9] in the crystal structure packing of alloxan showing preferential C=O···C=O contacts instead of hydrogen bonding between the acidic N–H and C=O.[10] In earlier crystallographic database studies, Taylor et al.[11] and Gavezzotti[12] have reported non-covalent interactions between pairs of carbonyl and cyano dipoles, and subsequently Allen et al.[13] carried out similar searches on the Cambridge Structural Database (CSD) and reported several favourable electrostatic C=O···C=O interactions. The authors described three configurations of idealised intermolecular carbonyl···carbonyl interaction geometries (Fig. 1); a slightly sheared anti-parallel, a highly sheared parallel, and a perpendicular motif, however they had diverse interpretations regarding the importance of these dipolar interactions on crystal packing. Several computational methods were accounted to elucidate the understanding of dipolar interactions[13–15]; more recently Lee et al.[16] published a more comprehensive CSD search on the role and importance of dipolar C=O···C=O interactions in crystal packing. From the analysis of structural data and computational studies, it was concluded that electrostatic energies are important in determining total interaction energies and geometries; however, steric repulsion and other intermolecular forces must also be considered.

Here we report the synthesis of two cyclic molecules: crown-3-pyromellitimide **4** and crown-6-bispyromellitimide **5**. Using mass spectrometry, we show that **4** binds preferentially to sodium over potassium ions while the opposite selectivity is observed for **5**. Infrared spectroscopy and single crystal X-ray diffraction analysis of **4** show unusual highly sheared anti-parallel dipolar carbonyl···carbonyl interactions. This novel CO···CO interaction mode opens up new avenues in the design and analysis of solid-state supramolecular systems and other areas of crystal engineering.

Results and Discussion

*Synthesis and Cation Recognition of Strapped Crown-3-Pyromellitimide **4** and Macrocyclic Crown-6-Bispyromellitimide **5***

Starting from pyromellitamide anhydride **1**, the synthesis of the target crown ether-pyromellitimide hybrids **4** and **5** was carried out in two simple steps as shown in Scheme 1. The pyromellitoyl

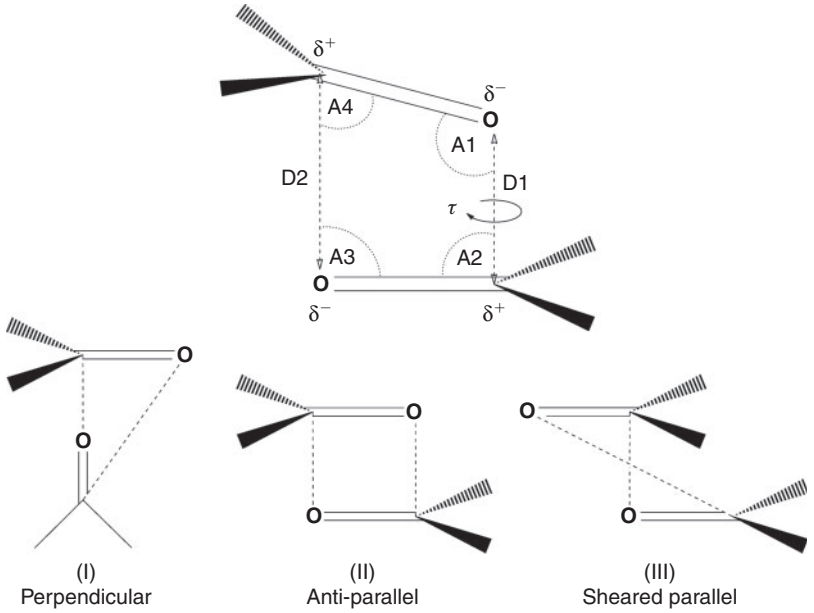

Fig. 1. The geometry and metric parameters of carbonyl···carbonyl interactions and the schematic drawings for three configurations of idealised intermolecular carbonyl···carbonyl interactions based on Allen and co-workers.[13]

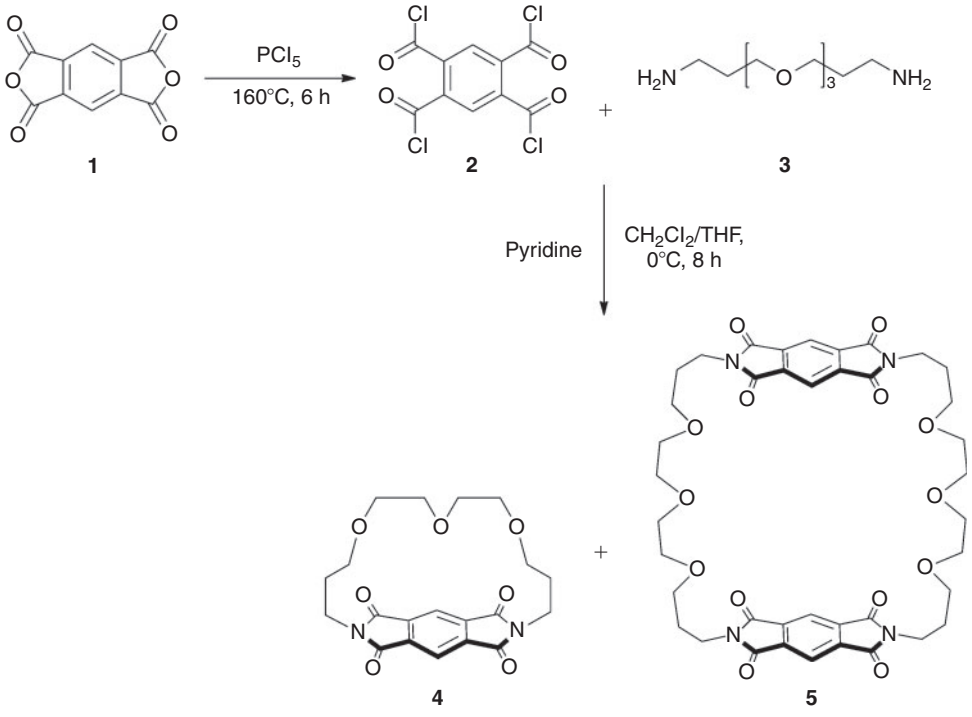

Scheme 1. Synthesis of crown-3-pyromellitimide **4** and crown-6-bispyromellitimide **5**.

chloride **2** was synthesised in 92 % yield according to the method reported by Baldwin and co-workers.[17] Subsequently, the acid chloride **2** was reacted with ethylene glycol diamine **3** in an anhydrous dichloromethane-tetrahydrofuran mixture at 0°C under high dilution to suppress polymerisation. Purification using silica chromatography yielded two novel cyclic compounds in 5 % yield for the strapped crown-3-pyromellitimide **4** and 1 % yield for macrocyclic crown-6-bispyromellitimide **5**.

The cation recognition capabilities of crown-3-pyromellitimide **4** and crown-6-bispyromellitimide **5** were investigated using orbitrap electrospray ionisation (ESI) high resolution mass spectrometry. The formation of adducts in the gas phase represents non-covalent interactions of the host-guest complex, providing a rapid screening method for the specificity and selectivity of molecular recognition.[18] Similar studies on the complexation of alkali metal cations with macrocyclic diamides using mass spectrometry were reported by Tarnowski et al.[19] Here, the size specificity of the smaller strapped crown-3-pyromellitimide **4** was demonstrated with the $\mathbf{4} \cdot Na^+$ host-guest complex ion formed in 23-times greater abundance

Table 1. Cation recognition selectivity of crown-3-pyromellitimide 4 and crown-6-bispyromellitimide 5 using HR-MS (ESI – see Supplementary Material)

Host	Cation	*m/z* Abundance ratio[A]
4	H^+	8.9
	Na^+	23
	K^+	1.0
	NH_4^+	8.2
5	H^+	1.0
	Na^+	17
	K^+	36
	NH_4^+	3.0

[A]The *m/z* abundance is normalised to the smallest $[M+X]^+$ peak observed after taking into account the relative isotope ratio of ^{14}N, ^{23}Na and ^{39}K.

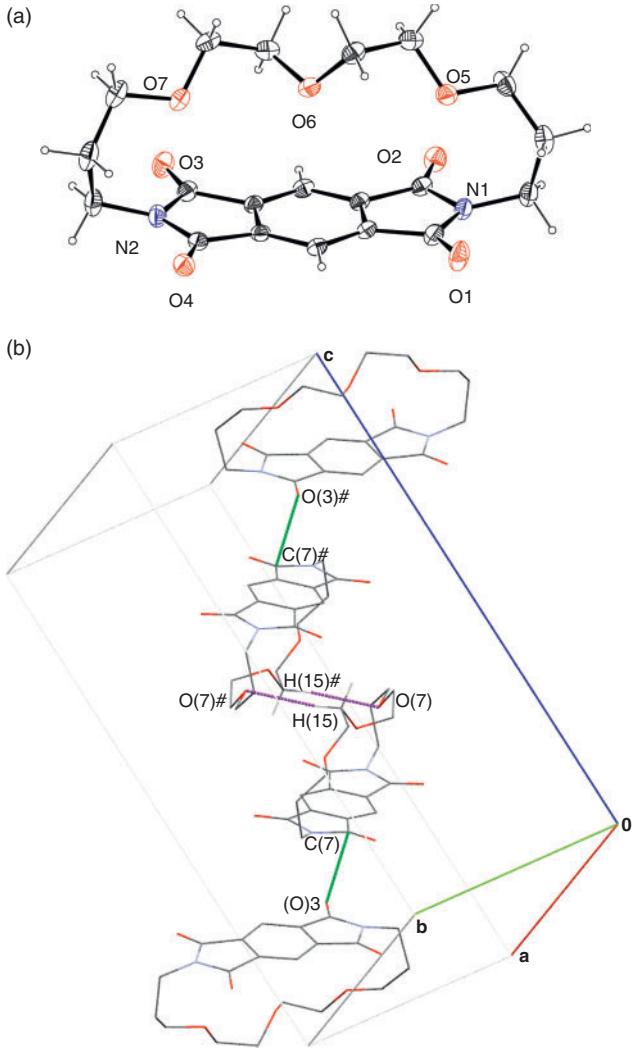

Fig. 2. Molecular structure of strapped crown-3-pyromellitimide **4** derived from single crystal X-ray analysis. (a) ORTEP diagram showing 50 % probability anisotropic displacement ellipsoids at 100 K, with H atoms drawn as circles with small radii. (b) Packing diagram within the unit cell (wireframe); all H atoms are omitted for clarity, except H(15) showing intermolecular hydrogen bonding. Dipolar carbonyl···carbonyl interactions: C=O···C=O (green dashed lines), glide plane symmetry: $1/2+x$, $1/2-y$, $1/2+z$. Hydrogen bonding C–H···O (purple dashed lines), inversion centre symmetry: $-x$, $-y$, $-z$.

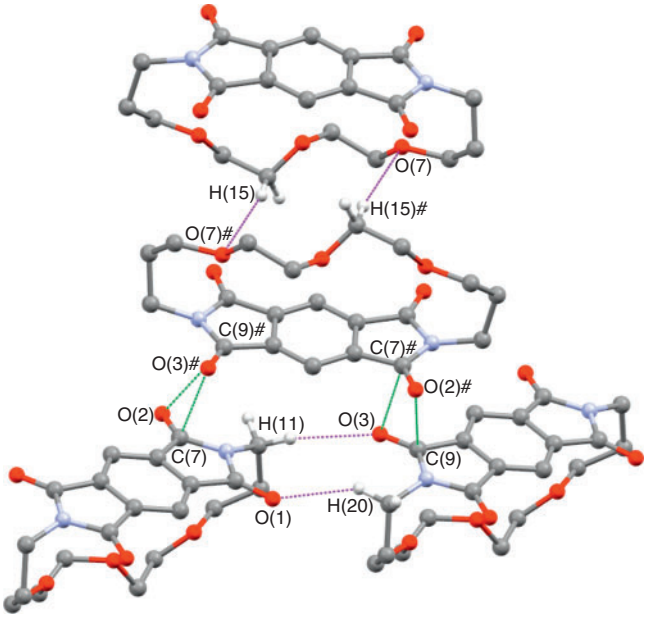

Fig. 3. Perspective packing diagram of compound **4** (ball and stick, 15 % van der Waals radii). All H atoms are omitted for clarity, except H(11), H(15), and H(20) showing intermolecular hydrogen bonding (purple dashed lines). Selected distances [Å] of intermolecular hydrogen bonding: O(7)···H(15) 2.579, O(1)···H(20) 2.555, O(3)···H(11) 2.617.

than the $\mathbf{4}\cdot K^+$ ion (Table 1). In contrast, crown-6-bispyromellitimide **5** appears to be less specific, with a modest 2-fold higher selectivity of K^+ over Na^+, consistent with well established 18-crown-6-ethers in the literature.

X-Ray Crystal Structure and Carbonyl··· Carbonyl Interactions of Strapped Crown-3-Pyromellitimide **4**

Single crystals of strapped crown-3-pyromellitimide **4** suitable for X-ray structure determination were grown by slow diffusion of diethyl ether into a solution of compound **4** in dichloromethane. Attempts to grow crystals of **5** have not been successful to date. The structure of crown-3-pyromellitimide **4** crystallises in the monoclinic space group $P2_1/n$ with the predicted molecular structure as shown in Fig. 2a. The crystal structure of *N*,*N*′-bis(2-methoxyethyl)pyromellitimide reported by Suchod et al.[20] demonstrated a perfect flat planar conformation of the centre pyromellitimide moiety. In contrast, a slight distortion in the flat plane (bending inwards) was observed in the molecular structure of compound **4**, which was interpreted as torsional strain on the cyclic structure, as expected for smaller macrocycles. Thus, the successful synthesis of this elegantly strapped crown-3-pyromellitamide **4** was remarkable given the unfavourable energetic strains involved in forming such a small macrocycle.

As shown in Fig. 2b, the packing diagram within the unit cell demonstrated two important intermolecular interactions responsible in the formation of the crystal lattice. The pyromellitic ‘face’ interacts via dipolar carbonyl···carbonyl interaction with a glide plane symmetry and an inversion centre symmetry of two molecules between the ‘straps’ through hydrogen bonding. Due to the poor H-donor nature of C–H, the unconventional hydrogen bonding interactions between molecules of compound **4** (i.e. CH···O, Fig. 3) are weaker (distance: 2.6 Å) compared with typical hydrogen bonds (distance: 1.6–2.0 Å)[21,22] with hydrogen covalently bonded to another electronegative atom.

Table 2. The key geometric parameters for intermolecular carbonyl···carbonyl interactions as defined in Fig. 1 for the three ideal C=O···C=O motifs[5] compared with those found in *N*,*N*′-bis(2-methoxyethyl)pyromellitimide (PMT)[20] and compound 4 (see Fig. 3, green dashed lines) in this study

	D1 [Å]	D2 [Å]	A1 [°]	A2 [°]	A3 [°]	A4 [°]	Torsion angle (τ) [°]	Conformation
Motif (I)[A]	3.02	–	75	15	180	90	0	Perpendicular
Motif (II)[A]	3.02	3.02	90	90	90	90	0	Anti-parallel
Motif (III)[A]	3.02	–	90	90	55	55	180	Sheared parallel
PMT[12][B]	3.111	3.128	96.3	84.5	95.5	83.4	0.8	Anti-parallel
Compound **4**[B]	3.178	3.452	80.4	106.3	68.3	92.5	44.1	Highly sheared anti-parallel

[A]Theoretical parameters resulting in minimum interaction energies [kJ mol^{-1}] from *ab initio* molecular-orbital calculations (6–31G** basis sets) as reported by Allen et al.[13]
[B]Measured values from X-ray crystallographic analysis.

Table 3. Correlation of intermolecular carbonyl···carbonyl interactions conformation to carbonyl bond distances and bond strengths from X-ray crystallographic and FT-IR spectroscopic data
ν_{as}: asymmetric stretch; ν_s: symmetric stretch

	C=O bond distances [Å]	C=O stretch	
		ν_{as} [cm^{-1}]	ν_s [cm^{-1}]
PMT[20,25]	1.204	1780	1710
Compound **4**	1.213	1765	1711
Compound **5**	–	1781	1718

The weak hydrogen bonding interaction suggests that the carbonyl···carbonyl interaction is the predominant driving force behind the crystal packing for crown-3-pyromellitimide **4**. Interestingly, the arrangement of the carbonyl···carbonyl interactions in compound **4** (Fig. 3) was observed to be significantly different from the reported non-cyclic *N*,*N*′-bis(2-methoxyethyl)pyromellitimide (PMT).[20] Herein, we discuss the three conformation motifs of intermolecular carbonyl···carbonyl interactions and their differences in the geometry and metric parameters in terms of the two C···O distances D1 and D2, four dihedral angles A1 to A4, and the torsion angle τ about the vectors of the two interacting carbonyl groups as shown in Fig. 3. Using *ab initio* molecular-orbital calculations (6–31G** basis sets) and applying the intermolecular perturbation theory (IMPT) to a bis-propanone dimer model, Allen et al.[13] established the ideal C···O distances (Table 2) for perpendicular and anti-parallel motifs with optimum interaction energies of -7.6 kJ mol^{-1} and -22.3 kJ mol^{-1} respectively.[23] This outcome is in agreement with the Cambridge Structural Database (CSD) study which reported the energetically favoured anti-parallel motif (II) is six times more common than the sheared parallel motif (III) and perpendicular motif (I).[13,23] The crystallographic analysis on the conformation of carbonyl···carbonyl interaction of the non-cyclic PMT[20] revealed an ideal anti-parallel motif (II) and the geometry parameters in Table 2 coincide with this observation. In comparison, the packing diagram of compound **4** in Fig. 3 demonstrated an unusual conformation, the geometry parameter listed in Table 2 resolves the conformation as a highly sheared anti-parallel motif (II) with a high torsion angle (τ: 44.1°). In respect to the CSD and theoretical study by Allen et al.[13] the occurrence of such high torsion angles in the anti-parallel (Motif II) carbonyl···carbonyl interaction is rare, and the calculated interaction energy where $\tau = 44.1°$ is approximately -15 kJ mol^{-1}.[13,24] The decline in the interaction energy can be correlated with the significant increase in the non-covalent C···O distances D1 and D2.

Further evidence for the high shearing effect comes from correlation of X-ray and IR spectroscopy data (Table 3), which shows elongation and weakening (red-shift) of the covalent C=O bond of compound **4**. In contrast, IR data for compound **5** indicated that the C=O bond strength is similar to the previously reported PMT, suggesting a minimal shearing effect on the intermolecular carbonyl···carbonyl interaction conformation, resembling the anti-parallel motif (II). The variations of conformation in these three different motifs provide a wide range of possible carbonyl···carbonyl interactions and in this discussion, we have demonstrated that the anti-parallel motif (I) can adopt a highly sheared anti-parallel conformation to accommodate the steric and torsion inflexibility of the strapped crown-3-pyromellitimide **4**.

Conclusions

We reported the synthesis of two novel cyclic molecules, the strapped crown-3-pyromellitimide **4** and macrocyclic crown-6-bispyromellitimide **5**, under high dilution condition. The selectivity of host-guest recognition of cations was demonstrated using high-resolution mass spectrometry (ESI), with compound **4** preferentially forming the $\mathbf{4}\cdot Na^+$ adduct and compound **5** favouring the $\mathbf{5}\cdot K^+$ adduct. In single crystal X-ray crystallography studies of the strapped crown-3-pyromellitimide **4**, two modes of supramolecular interaction were observed in the crystal packing; CH···O and carbonyl···carbonyl interactions. Further examination of the dipolar carbonyl···carbonyl interactions revealed an unusual highly sheared anti-parallel (Motif II) conformation in the crystal packing of compound **4**. In contrast the previously reported related non-cyclic PMT which also exhibits the anti-parallel motif (II), has a more commonly observed low torsion angle (τ: 0.8°). This suggests that the origin of the highly sheared anti-parallel carbonyl···carbonyl interaction in **4** is due to the strain imposed by the crown-ether strap upon the pyromellitimide core. Our findings could therefore be of considerable importance in crystal engineering as they highlight the importance of carbonyl···carbonyl interactions in the solid state even in cases such as for compound **4** that has to accomplish these via a high-shear angle between the carbonyl groups.

Experimental

General Methods and Materials

All starting materials were purchased from Sigma Aldrich. Pyromellitoyl chloride **2** was synthesised from pyromellitic dianhydride **1** according to a literature procedure.[17] Solvents and reagents were purchased from Sigma Aldrich, Merck, Ajax Finechem, and Honeywell Burdick & Jackson and used without further purification unless otherwise specified. Pyridine was purified by distillation and dried over potassium hydroxide. Anhydrous dichloromethane and tetrahydrofuran were dried and deoxygenated using a PureSolv MD-7 solvent purification system (Innovative Technology Inc.). Deuterated chloroform for NMR was purchased from Cambridge Isotope Laboratories. Column chromatography was performed using Davisil® chromatographic silica media (0.040–0.063 mm). Thin-layer chromatography was carried out using Merck Kieselgel 60 F-254 precoated sheets (0.25 mm).

All synthetic reactions were carried out in an inert environment containing nitrogen. Melting points were determined on a Mel-Temp II hot stage apparatus. Infrared spectra were recorded on a Thermo Scientific Nicolet Avatar 370 FT-IR spectrometer as a Nujol mull between sodium chloride plates. ^{1}H and ^{13}C NMR spectra were recorded on a Bruker Avance DPX 300 spectrometer operating at a frequency of 300.17 MHz for ^{1}H and 75.49 MHz for ^{13}C NMR respectively. NMR spectra were recorded at 298 K and samples were dissolved in $CDCl_3$; chemical shifts were referenced internally to residual solvent resonances (^{1}H: 7.26 ppm and ^{13}C: 77.16 ppm). Low resolution electrospray ionisation mass spectra were recorded on a Waters Micromass ZQ 2000 ESCi Multi-Mode Ionisation Source mass spectrometer equipped with *MassLynx 4.0* instrument software. High resolution ESI mass spectra were recorded on a Thermo Scientific Linear Quadrupole Ion Trap with Orbitrap Mass Analyser (LTQ ORBITRAP XL) mass spectrometer. Samples were acquired in electrospray ionisation mode using in-house made static glass nanospray tips inserted into a nanostage with 0.9 kV capillary voltage and FTMS setting at 60000 resolution, and the data then collected and processed with *Xcalibur 2.0* instrument software. Microanalysis was performed by the Research School of Chemistry, Australian National University, Canberra, Australia.

Synthesis of Crown-3-Pyromellitimide *4* and Crown-6-Bispyromellitimide *5*

A solution of pyromellitoyl chloride **2**[17] (2.98 g, 9.10 mmol) in anhydrous tetrahydrofuran (50 mL) and a solution of 4,7,10-trioxa-1,13-tridecanediamine **3** (4.02 g, 18.25 mmol) in anhydrous dichloromethane (50 mL) were added drop-wise into a stirred solution of anhydrous pyridine (2.93 g, 37.09 mmol), tetrahydrofuran (250 mL), and dichloromethane (250 mL) over a period of 8 h, maintained at 0°C in an ice bath. After addition was complete, the reaction mixture was stirred for 16 h at room temperature to afford a pale red solution with white precipitate. The solvent was removed *in vacuo* and the resultant brown residue was extracted with dichloromethane (3 × 30 mL) and the combined organic extracts were washed with aqueous hydrochloric acid (0.1 M, 50 mL), followed by water (50 mL) and then saturated aqueous sodium chloride (50 mL). The organic layer was dried over anhydrous magnesium sulfate, filtered, and concentrated under vacuum to afford the crude product as an orange residue. The crude product was purified by column chromatography over silica gel with methanol in dichloromethane (5 : 95 v/v) to remove polymeric compounds, and the eluent was concentrated under vacuum. This fraction was then further purified using column chromatography over silica gel with a gradient elution of methanol in dichloromethane (ranging from neat dichloromethane to methanol : dichloromethane, 5 : 95 v/v). A less polar fraction ($R_f = 0.78$) and a more polar fraction ($R_f = 0.27$) were collected; TLC (methanol : dichloromethane, 5 : 95 v/v).

The combined less polar fractions were evaporated to yield crown-3-pyromellitimide **4** as a white solid (193.5 mg, 5.3 %), m.p. 232–234°C; IR (Nujol) ν_{max}: 3072 (w), 3044 (w), 1765 (m), 1711 (s), 1461 (m), 1391 (m), 1093 (m), 726 (m) cm^{-1}; ^{1}H NMR (300.17 MHz, $CDCl_3$): δ 1.93–2.05 (m, 4H, $(NCH_2CH_2CH_2O)_2$), 2.77 and 3.03 (t, J 4.9 Hz, 8H, $(OCH_2CH_2O)_2$), 3.47 (t, J 4.8 Hz, 4H, $(NCH_2CH_2CH_2O)_2$), 3.95 (t, J 5.8 Hz, 4H, $(NCH_2)_2$), 8.26 (s, 2H, $(ArH)_2$); ^{13}C NMR (75.5 MHz, $CDCl_3$): δ 27.0 (CH_2), 37.8 (NCH_2), 70.3 (OCH_2), 71.0 (OCH_2), 71.1 (OCH_2), 118.1 (ArCH), 138.0 (ArC), 167.4 (C=O); MS (ESI): *m/z* 403.34 ($[M+H]^+$ requires 403.15); HR-MS (ESI): *m/z* 403.1506 ($[M+H]^+$, $C_{20}H_{23}N_2O_7$ requires 403.1505); Anal. Calcd. for $C_{20}H_{22}N_2O_7$: C, 59.70; H, 5.51; N, 6.96; O, 27.83. Found: C, 60.09; H, 5.33; N, 6.86; O, 27.72 %.

The combined more polar fractions were evaporated to yield crown-6-bispyromellitimide **5** as a white solid (32.7 mg, 0.5 %) m.p. 250–252°C; IR (Nujol) ν_{max}: 3069 (w), 3044 (w), 1781 (m), 1718 (s), 1456 (m), 1131 (m), 724 (m) cm^{-1}; ^{1}H NMR (300.17 MHz, $CDCl_3$): δ 1.92–2.03 (m, 8H, $(NCH_2CH_2CH_2O)_4$), 3.45–3.53 (m, 16H, $(OCH_2CH_2O)_4$, 3.55 (t, J 5.8 Hz, 8H, $(NCH_2CH_2CH_2O)_4$), 3.85 (t, J 7.0 Hz, 8H, $(NCH_2)_4$), 8.05 (s, 4H, $(ArH)_4$); ^{13}C NMR (75.5 MHz, $CDCl_3$): δ 28.6 (CH_2), 36.7 (NCH_2), 69.0 (OCH_2), 70.4 (OCH_2), 70.7 (OCH_2), 117.9 (ArCH), 137.4 (ArC), 166.4 (C=O); MS (ESI): *m/z* 843.62 ($[M+K]^+$ requires 843.89); HR-MS (ESI): *m/z* 805.2904 ($[M+H]^+$, $C_{40}H_{45}N_4O_{14}$ requires 805.2932); Anal. Calcd. for $C_{40}H_{44}N_4O_{14}$: C, 59.70; H, 5.51; N, 6.96; O, 27.83. Found: C, 59.53; H, 5.53; N, 6.63; O, 28.31 %.

X-Ray Structure Determination

The X-ray diffraction measurement for compound **4** was carried out on a Bruker kappa APEX-II CCD diffractometer at 150 K by using graphite-monochromated Mo-Kα radiation ($\lambda = 0.71075$ Å). The crystal was mounted on the goniometer using cryo loops for intensity measurements, was coated with paraffin oil, and then quickly transferred to the cold stream using an Oxford Cryostream 700 system attachment. Upon obtaining an initial refinement of unit cell parameters, the data collection strategy was worked out to achieve a redundancy of at least four throughout the resolution range (inf – 0.80 Å) at 10 s exposure time per frame making use of the kappa off sets on the four circle goniometer geometry. Data integration and reduction with the multi-scan absorption correction method was carried out using *Bruker APEX2 Suite* software.[26] The structure was solved by the Direct Methods program *SHELXS-97*[27] and refined by full-matrix least-squares refinement program *SHELXL*.[27] All non-hydrogen atoms were refined anisotropically and hydrogen atoms were included by using a riding model. Further crystal and refinement data are given in Table 4.

Crystallographic data (CCDC reference number 865686) can be obtained on request, free of charge, by quoting the publication citation and the deposition number via http://www.ccdc.cam.ac.uk/conts/retrieving.html, or from the Cambridge Crystallographic Data Centre, 12 Union Road,

Table 4. Summary of crystallographic and refinement data for compound 4

Mol. formula	$C_{20}H_{22}N_2O_7$
Mol. Weight	402.40
Crystal form	Colourless blocks
Crystal size [mm^3]	$0.29 \times 0.14 \times 0.08$
Temperature [K]	150(2)
Crystal system	Monoclinic
Space group	$P2_1/n$
a [Å]	8.2485 (10)
b [Å]	11.2813 (14)
c [Å]	20.512 (3)
α [°]	90
β [°]	97.562 (6)
γ [°]	90
Volume [Å^3]	1892.2 (4)
Z	4
D_c [g cm^{-3}]	1.413
μ(Mo-Kα) [mm^{-1}]	0.11
θ [°]	3.3–27.9
F(000)	848
Reflections collected	12320
Independent reflections	3290
Observed reflectionswith $I > 2\sigma(I)$	2442
Parameters varied	262
$\Delta\rho_{max}/\Delta\rho_{min}$ [e Å^{-3}]	0.16/−0.21
Restraint	0
Goodness-of-fit (F^2)	0.765
R_{int}	0.055
R_1 [$F^2 > 2\sigma(F^2)$]	0.039
$wR(F^2)$ (all data)[A]	0.131

[A] $w = 1/[\sigma^2(F_o^2) + (0.010P)^2]$ where $P = (F_o^2 + 2F_c^2)/3$.

Cambridge CB21EZ, UK; fax: (+44) 1223–336–033; or email: deposit@ccdc.cam.ac.uk.

Supplementary Material

Mass spectra for the cation recognition selectivity studies shown in Table 1 are available on the Journal's website.

Acknowledgements

The authors thank the facilities of the Mark Wainwright Analytical Centre of the University of New South Wales. We acknowledge the Australian Research Council for a Discovery Project Grant (DP09855059) to P. T. and the Australian Government and University of New South Wales for a Ph.D. scholarship to ENWH.

References

[1] J.-M. Lehn, *Angew. Chem. Int. Edit.* **1988**, *27*, 89. doi:10.1002/ANIE.198800891

[2] R. Paulini, K. Müller, F. Diederich, *Angew. Chem. Int. Edit.* **2005**, *44*, 1788. doi:10.1002/ANIE.200462213

[3] C.-Q. Wan, T. C. W. Mak, *Cryst. Growth Des.* **2011**, *11*, 832. doi:10.1021/CG101490A

[4] H.-J. Böhm, G. Klebe, *Angew. Chem. Int. Edit.* **1996**, *35*, 2588. doi:10.1002/ANIE.199625881

[5] C. Fäh, L. A. Hardegger, M.-O. Ebert, W. B. Schweizer, F. Diederich, *Chem. Commun. (Camb.)* **2010**, *46*, 67. doi:10.1039/B912721F

[6] C. M. Deane, F. H. Allen, R. Taylor, T. L. Blundell, *Protein Eng.* **1999**, *12*, 1025. doi:10.1093/PROTEIN/12.12.1025

[7] R. Carrillo, M. López-Rodríguez, V. S. Martín, T. Martín, *CrystEngComm* **2010**, *12*, 3676. doi:10.1039/C001261K

[8] W. Bolton, *Acta Crystallogr.* **1963**, *16*, 166. doi:10.1107/S0365110X63000438

[9] W. Bolton, *Acta Crystallogr.* **1965**, *18*, 5. doi:10.1107/S0365110X65000026

[10] W. Bolton, *Acta Crystallogr.* **1964**, *17*, 147. doi:10.1107/S0365110X6400041X

[11] R. Taylor, A. Mullaley, G. W. Mullier, *Pestic. Sci.* **1990**, *29*, 197. doi:10.1002/PS.2780290209

[12] A. Gavezzotti, *J. Phys. Chem.* **1990**, *94*, 4319. doi:10.1021/J100373A081

[13] F. H. Allen, C. A. Baalham, J. P. M. Lommerse, P. R. Raithby, *Acta Crystallogr. B* **1998**, *54*, 320. doi:10.1107/S0108768198001463

[14] F. R. Fischer, P. A. Wood, F. H. Allen, F. Diederich, *Proc. Natl. Acad. Sci. USA* **2008**, *105*, 17290. doi:10.1073/PNAS.0806129105

[15] H. A. Sparkes, P. R. Raithby, E. Clot, G. P. Shields, J. A. Chisholm, F. H. Allen, *CrystEngComm* **2006**, *8*, 563. doi:10.1039/B607531M

[16] S. Lee, A. B. Mallik, D. C. Fredrickson, *Cryst. Growth Des.* **2004**, *4*, 279. doi:10.1021/CG0300228

[17] J. Almog, J. E. Baldwin, M. J. Crossley, J. F. Debernardis, R. L. Dyer, J. R. Huff, M. K. Peters, *Tetrahedron* **1981**, *37*, 3589. doi:10.1016/S0040-4020(01)98887-8

[18] M. Vincenti, *J. Mass Spectrom.* **1995**, *30*, 925. doi:10.1002/JMS.1190300702

[19] P. Tarnowski, W. Danikiewicz, J. Jurczak, *Pol. J. Chem.* **2004**, *78*, 927.

[20] B. Suchod, J. P. Curtet, D. Djurado, M. Armand, *Acta Crystallogr. C* **1999**, *55*, 445. doi:10.1107/S0108270198013997

[21] G. R. Desiraju, T. Steiner, *The Weak Hydrogen Bond in Structural Chemistry and Biology* **1999** (Oxford University Press: New York, NY).

[22] G. A. Jeffrey, *An Introduction to Hydrogen Bonding* **1997** (Oxford University Press: New York, NY).

[23] Since the sheared parallel motif (III) also exhibits only one non-covalent C···O interaction, the authors in [13] viewed that it is reasonable to assume that the interaction energy for motif (III) is similar to that in the perpendicular motif (I). The author also acknowledged the oxygen atoms of the two carbonyl groups in motif (III) are both exposed, hence the oxygen atoms can take part in further interactions to enhance the overall interaction energy, which could be the underlying cause for the slightly greater occurrence of motif (III) compared to motif (I).

[24] The authors in [13] carried out the IMPT calculations with the torsion angle τ varied from 0° to 90° with fixed D1 and D2 values of 3.02 Å. There was a very small increase in the interaction energies over the range of $\tau = 0°$ to 30°, from −22.3 to −19.1 kJ mol^{-1}. However, the energy increases rapidly and becomes repulsive at $\tau > 70°$.

[25] B. O. Linn, L. M. Paege, P. J. Doherty, R. J. Bochis, F. S. Waksmunski, P. Kulsa, M. H. Fisher, *J. Agric. Food Chem.* **1982**, *30*, 1236. doi:10.1021/JF00114A058

[26] *Bruker APEX2 Suite* **2007** (Bruker AXS Inc.: Madison, WI).

[27] G. Sheldrick, *Acta Crystallogr. A* **2008**, *64*, 112. doi:10.1107/S0108767307043930